

The Evolution and Luminosity Function of Quasars

Vahé Petrosian

Center for Space Science and Astrophysics, Varian 302c, Stanford University, Stanford, CA, 94305-4060

Abstract. I report results from analysis of data from several quasar samples (Durham/AAT, LBQS, HBQS and EQS) on the density and the luminosity evolution of quasars. We have used new statistical methods whereby we combine these different samples with varying selection criteria and multiple truncations. With these methods the luminosity evolution can be found through an investigation of the correlation of the bivariate distribution of luminosities and redshifts. Of the two most commonly used models for luminosity evolution, $L = e^{kt(z)}$ and $L = (1+z)^{k'}$, we find that the second form, with $k' = 2.58$ (one σ range [2.14, 2.91]), gives a better description of the data at all luminosities. Using this form of luminosity evolution we determine a global luminosity function and the evolution of the co-moving density for the two classes of cosmological models. We find a gradual increase of the co-moving density up to $z \sim 2$, at which point the density peaks and begins to decrease rapidly. This is in agreement with results from high redshift surveys and in disagreement with the pure luminosity evolution (i.e. constant co-moving density) model. We find that the local luminosity function exhibits the usual double power law behavior. The luminosity density is found to increase rapidly at low redshift and to reach a peak at around $z \approx 2$. This result is compared with those from high redshift surveys and with the evolution of the star formation rate.

1. Introduction

This work is an outcome of collaborations with Professor Bradly Efron of Department of Statistics and Alexander Maloney, a student at Department of Physics at Stanford University. A more complete description of this work can be found in Efron & Petrosian (1999) and Maloney & Petrosian (1999).

The first aim of this work is to determine the so called **statistical evolution** of quasars and other active galactic nuclei (AGNs) as described by the luminosity function and its variation with cosmic time t or redshift z ; $\Psi(L, z)$. This evolution is different than what one may call the **physical evolution** (see, e.g. Lynds & Petrosian 1972) such as the rate of formation or birth of sources as a function of cosmological epoch, $S(L, z)$, and the rate of the variation of the luminosities, $L(z)$ or $\dot{L} = dL/dz$. These two types of evolutions are connected via the continuity equation (see, e.g. Cavaliere & Padovani 1988; Caditz & Petrosian 1990):

$$\partial\Psi(L, z)/\partial z + \partial(\dot{L}\Psi(L, Z))/\partial L = S(L, z). \quad (1)$$

The ultimate goal is to relate the physical evolution functions to the models for production of the luminosity (see, e.g. Caditz, Petrosian & Wandel 1991) and other cosmic evolutionary processes.

Investigations of the statistical evolution of the quasar have played a major role in the development of our ideas about these sources. From the very beginning (Schmidt 1968, and Lynds and Wills 1972) it has been evident that quasars have undergone rapid evolution which was then described by the pure density evolution (PDE) models; $\Psi(L, z) = \psi(L)\rho(z)$, with $\rho(z)$ describing the co-moving density evolution. However, both the source counts and the redshift distribution of optically selected samples of quasars (see e.g. Marshall 1985) clearly showed that PDE cannot be correct and favored the pure luminosity evolution (PLE) model, with $\Psi(L, z) = \psi(L/g(z))/g(z)$. The function $g(z)$ (with $g(0) = 1$) describes the luminosity evolution of the population with $L_o = L/g(z)$ as the luminosity adjusted to its present epoch value. As we shall see below, this model also appears to be inadequate.

Without loss of generality, we can write the luminosity function as

$$\Psi(L, z) = \rho(z)\psi(L/g(z), \alpha_i)/g(z), \quad (2)$$

where $\psi(L_o, \alpha_i)$ gives the local luminosity function. Here we explicitly include the shape parameters α_i , which could also vary with redshift. A surprising result has been the absence of evidence for strong shape variation so in this paper we ignore these variations.

In the next section we give a brief description of the new statistical methods we have developed for accurate determination of $\Psi(L, z)$. In §3 we list the characteristics of the data used for this purpose and in §4 we present the results.

2. The Statistical Methods

The presence of the function $g(z)$ implies that the variables L and z may be correlated. The statistical problem at hand is to first determine the degree of this **correlation** and then determine the univariate **distributions** $\rho(z)$ and $\psi(L_o)$ from an observed bivariate distribution which suffers from selection biases and is subject to multiple truncations. The left panel of Figure 1 shows some generic truncations. The distribution may be truncated parallel to the axis (dotted lines) which can be referred to as untruncated because there is no bias within the observed ranges. More interesting cases are when the truncation is not parallel to the axis. The data may suffer a one-sided truncation from below (solid curve) or above (dashed curve), truncated both from above **and** below or in a more complex way. The most general truncation is when each data point, say $[L_i, z_i]$, has its individual upper or lower limits, $L_i^- < L_i < L_i^+$ and $z_i^- < z_i < z_i^+$, as shown by the large cross for one point. In several papers (Petrosian 1992, Efron & Petrosian 1992 and 1998) we have developed new methods for dealing with all of these situations. These are essentially non-parametric methods which avoid the usual arbitrary binning and the consequent loss of data.

Briefly, the determination of the correlation (i.e. the luminosity evolution) function $g(z)$ is based on the rank order R_i of each source among its *comparable*

or eligible set $J_i = \{j : y_j > y_i, y_j \in (y_i^-, y_i^+)\}$, where y stands for either variable. One then defines the test statistic $\tau = \sum_i (R_i - E_i) / \sqrt{\sum_i V_i}$ with $E_i = \frac{1}{2}(N_i + 1)$ and $V_i = \frac{1}{12}(N_i^2 - 1)$, where N_i is the number of points in J_i . This statistic is equivalent to Kendall's τ test and for independent variables its distribution should be a gaussian with mean of zero and dispersion of unity. Thus, the luminosity and redshift will be uncorrelated or stochastically independent if $|\tau| < 1$, in which case one may assume that there is no luminosity evolution ($g(z) = 1$) and proceed with the determination of the univariate distributions $\psi(L)$ and $\rho(z)$ using the methods mentioned below. However, if $|\tau| \geq 1$ then L and z cannot be considered independent and one may assume that the most likely explanation is the presence of luminosity evolution ($g(z) \neq \text{constant}$). One can then determine the function $g(z)$ parametrically as follows.

Given a parametric form for the luminosity evolution $g_k(z)$ one can transform the luminosities into $L_o(k) = L/g_k(z)$ and proceed with the determination of the test statistic $\tau(k)$ for the new variables L_o and z as a function of k . The most likely value of k is that with $\tau(k) = 0$ and the range of k for 1 σ confidence level is $\{k : |\tau(k)| < 1\}$. The right panel of Figure 1 shows an example of our results using this procedure.

The last step is the determination of the univariate distributions $\psi(L_o)$ and $\rho(z)$ with our methods which are generalizations of Lynden-Bell's (1971) C^- method.

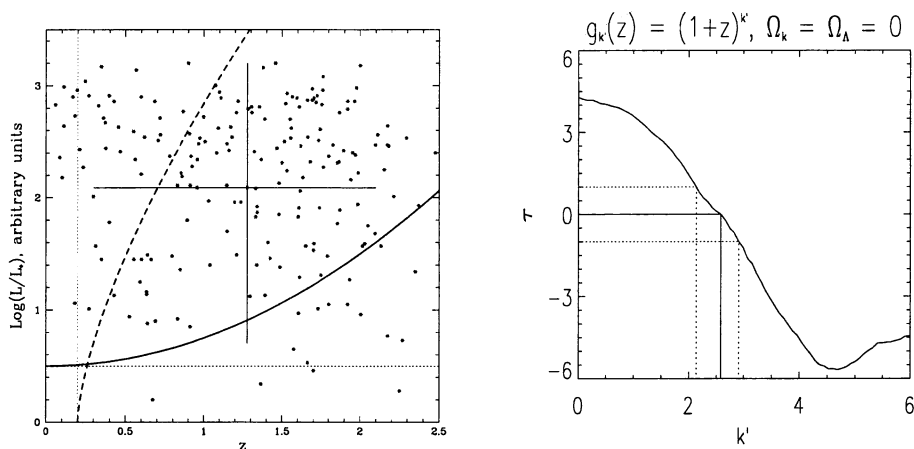


Figure 1. Left Panel: Demonstration of various types of data truncations: Parallel to axis (dotted lines), from below (the solid curve), from above (the dashed curve), and a general truncation when each data point has its specific observable range (shown by the cross for only one of the points). Right Panel: A determination of the luminosity evolution parameter for the parametric form $g_{k'}(z) = (1+z)^{k'}$. The correlation statistic τ is shown as a function of k' for the combined data set for the Einstein - de Sitter cosmological model. The solid line at $\tau = 0$ gives the optimal value $k' = 2.58$ and the dotted lines at $|\tau| = 1$ demonstrate the 1 σ range [2.14, 2.91].

3. The Data

The redshifts and B magnitudes of the data used here are shown in Figure 2. It includes the Large Bright QSO survey (LBQS) containing 1055 QSOs in the magnitude range $16.0 < B_J < 18.85$ and redshift range $0.2 < z < 3.4$ (Hewett et al. 1995) and the Homogeneous Bright QSO Survey (HBQS) (Cristiani et al. 1995) with 285 QSOs in the range $15.5 < B_J < (18.25 \text{ to } 18.85)$ and $0.3 < z < 2.2$. The lower cluster of dots in Figure 2 show the above two data sets in the $0.3 < z < 2.2$ range. The upper cluster of points show the Durham/AAT survey containing 419 QSOs in the magnitude range $17.0 < b < 21.27$ (Boyle et al. 1990) and redshift range $0.3 < z < 2.2$, giving information about the QSO luminosity function in a different regime than the previous two samples. Finally we have added the crosses, a subsample of the Edinburgh QSO Survey (EQS) consisting of 8 QSOs brighter than $B = 16.5$ that fall in the redshift range $0.3 < z < 2.2$ (Goldschmidt et al. in 1992), and give information about the luminosity function at the bright end.

There have been several previous analyses of the above surveys (Boyle et al. 1992, La Franca & Cristiani 1996, Hatziminaoglou et al. 1998) using binning and PLE or PDE models. Our approach is unique in that we combine all of these data and determine both the luminosity and density evolution laws independently.

Before presenting our results we briefly discuss the QSO Hubble diagram and the question of the non-cosmological origin of their redshifts.

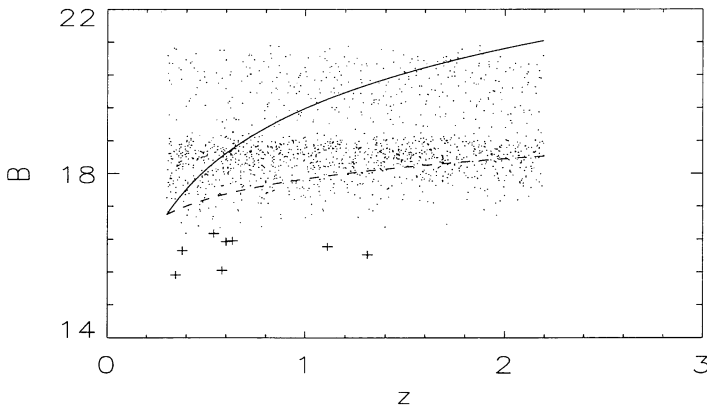


Figure 2. The B magnitude - redshift data for the four samples LBQS and HBQS (lower cluster), Durham/AAT (upper cluster), and EQS (crosses) for $0.3 < z < 2.2$. The data are fitted to the parametric form $B(z) = B_o - \beta \log(d_L^2(z)K(z)) + \text{constant}$. The best fit ($\beta = 0.84$) is shown by the dashed line. The solid line shows the expected relation between B and z for standard candles ($\beta = 2.5$). We have used the Einstein-de Sitter model.

3.1. The Quasar Hubble Diagram

At first glance there does not seem to be clear evidence for a Hubble type relation in Figure 2. This well known result has been used as an argument against the cosmological origin of quasar redshifts (see, e.g. Burbidge & O'Dell 1973). However, this is not the only possible interpretation. One would not expect a simple Hubble diagram for sources with a broad luminosity function (nonstandard candles, see e.g. Petrosian 1974). The absence of an obvious Hubble relation can also arise from approximate cancellation between cosmological dimming and luminosity evolution. Exact cancellation of these two effects is highly implausible and could bring into question the basic assumptions about the distribution of quasars. To clarify this situation we have applied the correlation tests described in §2 to the combined data and find a correlation with $\tau = 3.63$. This result rejects the hypothesis of independence between B and z at the 99.97% confidence level. In addition, given a cosmological model with parameters Ω_i , we may test the parametric fit $B(z) = B_o - \beta \log(d_L^2(z, \Omega_i)K(z)) + \text{constant}$, where d_L is the luminosity distance and $K(z)$ is the K-correction term. We find that for the Einstein - de Sitter model $B(z)$ and z are uncorrelated, i.e. $\tau(\beta) = 0$, for $\beta = 0.84$, which is shown by the dashed line in Figure 2. Here we also show the expected relation for standard candles ($\beta = 2.5$, the solid line). This results shows that β , while clearly less than 2.5, differs significantly from the value of zero expected in case of the complete absence of a Hubble relation or the exact cancellation described above.

We now turn to the determination of the evolution of the luminosity function. We have used two classes of cosmological models; models with zero cosmological constant Λ or $\Omega_\Lambda = \Lambda/3H_o^2 = 0$, and flat or inflationary models with non-zero cosmological constant or $\Omega_k \equiv 1 - \Omega_M - \Omega_\Lambda = 0$. Here Ω_M is the matter density parameter and $H_o = 70 \text{ km}/(\text{s Mpc})$ is our assumed value of the Hubble constant, although most results are independent of this assumption. Here we present our results for the Einstein-de Sitter model ($\Omega_\Lambda = \Omega_k = 0$). The other models give qualitatively similar results.

4. The Results

The results we have obtained can be summarized as follows:

- We find a strong **correlation** between luminosity and redshift, indicating presence of a rapid luminosity evolution.
- For determination of the **Luminosity evolution** we examine the two commonly used forms: the power law $g(z) = (1+z)^{k'}$ and the exponential $g(z) = e^{kt(z)}$, where $t(z)$ is the fractional lookback time. We find that the first form provides a better description of the data than the second. We find the value of $k' = 3.53$ for the Durham/AAT sample which is similar to the values found by others (3.45, Boyle 1992; 3.2, Caditz & Petrosian 1990). However, the value 2.58 that we obtain for the combined data is smaller than the previous estimates (e.g. 3.26, La Franca & Cristiani 1996) most of which assume a pure luminosity evolution, i.e. a constant $\rho(z)$. The exponent k' of the luminosity evolution is somewhat coupled to the strength of the density evolution (see also below). An incorrect assumption about the latter will result in an incorrect value for k' . In

our method we obtain k' without any assumptions about the form or strength of the density evolution.

In order to better model this evolution future analyses of quasar evolution could consider parametric forms, with more than one free parameter. More complex forms of luminosity evolution have sometimes been expressed in terms of a luminosity dependent luminosity (or density) evolution. These forms can be turned into a simple luminosity *independent* luminosity evolution form with more than one parameter. For example, the form with the exponent $k' = k_1 - k_2(z)\ln(L/L_*)$ for $L > L_*$ used by La Franca & Cristiani (1996) is the same as the simpler luminosity independent luminosity evolution with $k' = k_1/[1 + k_2\ln((1+z)/(1+z_*))]$ for z greater than some z_* .

Given the form of the luminosity evolution we make the simple transformation of all luminosities to their hypothetical present epoch values, $L_0 = L/g(z)$, so that L_0 and z are uncorrelated. This allows us to use our methods to determine the **univariate distributions** of z and L_0 .

- We find that the **co-moving density evolution** depends somewhat on the cosmological model. As shown in the left panel of Figure 3 our results show a relatively slow increase ($\rho \sim (1+z)^{2.5}$) for low redshifts and a rapid decline ($\rho \sim (1+z)^{-5}$) for $z > 2$, which is similar to the high redshift results from Schmidt et al. (1995) and Warren et al. (1994). These exponents are very approximate because, as evident in this figure, power laws are not good representations of the results.

As mentioned above the values of these exponents are coupled to the parameters describing the luminosity evolution. A higher value of k' would give a slower density evolution for $z < 2$. For example, Caditz & Petrosian (1990) use a higher value of k' and find a constant or slowly decreasing co-moving density. Similarly, previous analyses (e.g. Schmidt 1968) assuming no luminosity evolution ($k' = 0$) have consistently given a large (> 5) value for the exponent of the pure density evolution power-law. Miyaji, Hasinger & Schmidt (1998) make the same assumption and find similar results for the soft X-ray luminosity function. On the other hand, we find that the decline of the co-moving density for $z > 2$ is steeper than the previous results for both the optical luminosity function (Schmidt et al. 1995 and Warren et al. 1994) and the soft X-ray luminosity function (the constant $\rho(z)$ results of Miyaji et al. 1998). This is partly due to the assumption of pure density evolution in all three of these previous works and partly due to the incompleteness at high redshift of the data used in our analysis.

- We find that the **cumulative local luminosity function**

$$\Phi(L_0) = \int_{L_0}^{\infty} \psi(x) dx$$

can be described by a double power law form found previously. Our values for the low and high luminosity power law indices, $k_1 = 1.05$ and $k_2 = 3.17$, are consistent with values of 1.35 to 1.50 and 3.6 to 3.9 obtained previously (Caditz & Petrosian 1990, La Franca & Cristiani 1996). There appears to be little variation with redshift of the shape of the cumulative and differential luminosity functions, thus the $\alpha_i = \text{constant}$ prescription [see eq. (2)] seems adequate.

- The above results allow us to determine the **luminosity density evolution** $\mathcal{L}(z) \propto \rho(z)g(z)$. As shown in the right panel of Figure 3, this measure increases rapidly with z at low redshift, peaks around $z \approx 2$ and then decreases.

Here we have included all of the LBQS data extending to $z = 3.3$ and the high redshift survey quasars (Schmidt et al. 1995, Warren et al. 1994). It has been claimed (Cavaliere & Vittorini 1998, Shaver et al. 1998) that this rise and fall of $\mathcal{L}(z)$ with redshift is similar to the behavior of the star formation rate (SFR), which has recently been extended to high redshifts (see, e.g. Madau 1997, and Hughes et al. 1998, from SCUBA, presented also in these proceedings). We have shown these rates in the above figure as well. Although the general trends of rise and fall of the SFR and $\mathcal{L}(z)$ are similar, there is considerable difference in the detailed variations. (Our quasar results seem to be in better agreement with the SCUBA than the Madau results.) The similarity may indicate some relation between the SFR and the feeding of the central engine of the quasars (e.g. both are affected by mergers). However, considering the many differences between the star formation process and the generation of energy in quasars the above differences are not surprising.

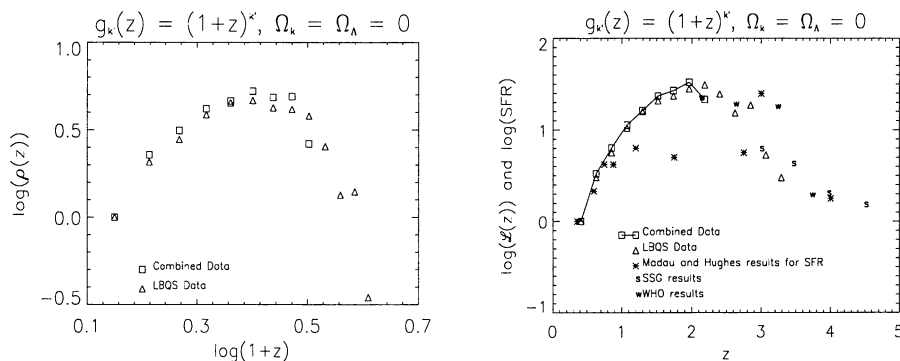


Figure 3. Left Panel: The density evolution $\rho(z)$ vs redshift for the Einstein - de Sitter cosmological model. Clearly, neither the pure luminosity evolution model with $\rho(z) = \text{const.}$, nor a simple evolutionary form $\rho \propto (1+z)^\mu$ will be adequate to describe the density evolution. The squares show the results for the combined data in the region $0.3 < z < 2.2$ and the triangles show the results for the LBQS data in the region $0.3 < z < 3.3$. Right Panel: The luminosity density $\mathcal{L}(z)$ vs redshift for the Einstein - de Sitter model. The squares and triangles give our results for the combined data and the LBQS data, respectively. The high redshift results of Schmidt et al. (1995) and Warren et al. (1994) are given by the letters “s” and “w”, respectively. The vertical normalizations are arbitrary. All of the above results indicate that \mathcal{L} peaks somewhere in the region $z \approx 2$. The star formation rate (SFR) as a function of redshift, as found by Madau (1997) and Hughes et al. (1998), is given by the asterisks. The results of Hughes et al. (the point at $z = 3$ which in reality extends from $z = 2$ to 4) give a much higher SFR at high redshift than the results of Madau and is in better agreement with the quasar results.

References

- Boyle, B. J., Fong, R., Shanks, T., & Peterson, B. A. 1990, M.N.R.A.S., 243, 1.
- Boyle, B. J. 1992, in *Texas/ESO-CERN Symp. on Rel. Astro., Cosmology and Particle Physics*, eds. Barrow, J. D., Mestel, L. & Thomas, P., Ann. N. Y. Acad. of Sci., 647, 14.
- Burbidge, G. R., & O'Dell, S.L. 1973, Ap.J., 183, 759.
- Caditz, D., & Petrosian, V. 1990, Ap.J., 357, 326.
- Caditz, D., Petrosian, V., & Wandel, A. 1991, Ap. J. (Letters), 372, L63.
- Cavaliere, A., & Padovani, P. 1988, Ap.J. (Letters), 333, L33.
- Cavaliere, A., & Vittorini, V. 1998, to appear in *The Young Universe*, Eds. S. D'Odorico, A. Fontana & E. Giallongo ASP Conf. Series 1998, v2; astro-ph/9802320.
- Cristiani, S., La Franca, F., & Andreani, P., et al. 1995, A. & A. Suppl., 112, 347.
- Efron, B., & Petrosian, V. 1992, Ap.J., 399, 345.
- Efron, B., & Petrosian, V. 1998, JASA, in press; astro-ph/9808334.
- Goldschmidt, P., Miller, L., La France, F., & Cristiani, S. 1992, M.N.R.A.S., 256, 65.
- Hatziminaoglou, E., Van Waerbeke, L. & Mathez, G. 1998,
- Hewett, P. C., Foltz, C. B., & Chaffee, F. H. 1995, A.J., 109, 1498.
- Hughes, D. H. et al. 1998, Nature, 394, 241
- La Franca, F., & Cristiani, S. 1996, invited talk in *Wide Field Spectroscopy* (20-24 May 1996, Athens), Eds. M. Kontizas et al.; astro-ph/9610017.
- Lynden-Bell, D. 1971, M.N.R.A.S., 155, 95.
- Lynds, R. C., & Petrosian, V. 1972, Ap.J., 175, 591.
- Lynds, R. C., & Wills, D. 1972, Ap.J., 175, 531.
- Madau, P. 1997, to appear in *The Hubble Deep Field*, Eds. M. Livio, S. M. Fall, & P. Madau, STScI Symposium Series; astro-ph/9709147.
- Maloney, A. & Petrosian, V. 1999, Ap.J., in press, vol 518; astro-ph/9807166.
- Marshall, H. L. 1985, Ap.J., 299, 109.
- Miyaji, T. Husinger, G. & Schmidt, M. 1998, astro-ph/9809398.
- Petrosian, V. 1974, Ap.J., 188, 443.
- Petrosian, V. 1992, in *Statistical Challenges in Modern Astronomy*, Eds. E. D. Feigelson & G. J. Babu, (New York: Springer-Verlag), p. 173.
- Schmidt, M. 1968, Ap.J., 151, 393.
- Schmidt M., Schneider, D. P. & Gunn, J. E. 1995, A.J., 110, 68.
- Shaver, P.A., Hook, I. M., Jackson, C. A., Wall, J. V., & Kellermann, K. I. 1998, to appear in *Highly Redshifted Radio Lines*, eds. C. Carilli, S. Radford, K. Menten, G. Langston, (PASP: San Francisco); astro-ph/9801211.
- Warren, S. J., Hewett, P. C., & Osmer, P. S. 1994, Ap.J., 421, 412.